

Cooperative Multi-Agent Actor-Critic for Privacy-Preserving Load Scheduling in a Residential Microgrid

Zhaoming Qin, *Student Member, IEEE*, Nanqing Dong, Eric P. Xing, *Fellow, IEEE*,
and Junwei Cao, *Senior Member, IEEE*

Abstract—As a scalable data-driven approach, multi-agent reinforcement learning (MARL) has made remarkable advances in solving the cooperative residential load scheduling problems. However, the common centralized training strategy of MARL algorithms raises privacy risks for involved households. In this work, we propose a privacy-preserving multi-agent actor-critic framework where the decentralized actors are trained with distributed critics, such that both the decentralized execution and the distributed training do not require the global state information. The proposed framework can preserve the privacy of the households while simultaneously learn the multi-agent credit assignment mechanism implicitly. The simulation experiments demonstrate that the proposed framework significantly outperforms the existing privacy-preserving actor-critic framework, and can achieve comparable performance to the state-of-the-art actor-critic framework without privacy constraints.

Index Terms—Actor-critic, load scheduling, multi-agent reinforcement learning, privacy-preserving.

I. INTRODUCTION

A. Motivation

As ultimate consumers in the electricity transmission chain, residential loads account for nearly 40% of total electricity consumption in the developed countries (e.g., about 37.8% in the U.S. in 2019 [1]). The large flexibility of residential loads provides a great potential for energy regulation and scheduling, promoting the vigorous development of smart homes [2]. By integrating multiple smart homes, the residential microgrid can aggregate the capacity of load scheduling and reduce the total energy costs. So far, the load scheduling of the residential microgrid has gained increasing attention [3], [4], [5].

In recent years, the breakthroughs in multi-agent reinforcement learning (MARL) have led to new solutions to the load scheduling problem [6]. First, the residential microgrid with multiple households is naturally modeled as a multi-agent environment where each household is an agent. Second,

without any prior knowledge of the residential microgrid, the model-free reinforcement learning (RL) can learn practical policies by interacting with the environment and perform real-time execution based on the learned policies [7].

Although the massive effort has been dedicated to developing the cooperative load scheduling schemes using MARL [8], [9], [10], [11], [12], few of these studies focus on the privacy issues. During the training of MARL, the access to the information of households may breach the user privacy. For example, the behaviors of the occupants can be captured from the arrival and departure time of the household electric vehicle (EV) [13]. Another case is that occupants' temperature preference can be inferred from the thermal comfort constraints [14]. Therefore, it is essential to develop a privacy-preserving MARL framework to address the cooperative load scheduling problem.

B. Literature Review

To this end, several MARL frameworks have been developed [15], [16]. A simple framework is to integrate all agents as a single agent with joint state space and action space, where a single-agent RL algorithm is applied [17]. For instance, a *centralized actor-critic* (CAC) framework using prioritized deep deterministic policy gradient (DDPG) is employed to manage all devices of a residential multi-energy system [18]. Although this centralized framework theoretically allows the cooperative behaviours across agents, it fails on simple cooperative MARL problems due to *lazy* agents in practice [19]. Furthermore, the joint action space of the agents increases exponentially with the number of agents, resulting in poor scalability [20]. Additionally, the centralized framework needs to collect observations from individual agents and distribute actions to them. This relies on high-quality real-time communication and poses a threat to the privacy of the agents.

Above-mentioned constraints necessitate the decentralized policies that depend only on agents' local observations. A straightforward framework to learn decentralized policies is to train the agents independently [15]. For example, an *independent actor-critic* (IAC) framework using proximal policy optimization (PPO) approach is adopted to optimize a multi-household energy management scheme [8]. The independent Q-learning is applied to the demand response programs for different components in residential buildings [21]. From the perspective of a single agent in such a framework, the behaviours and policies of other agents cannot be captured [16].

The first two authors contributed equally to this work.

Z. Qin is with the Department of Automation, Tsinghua University, Beijing 100084, China.

N. Dong is with the Department of Computer Science, University of Oxford, Oxford, OX1 3QD, UK.

E. P. Xing is with the Machine Learning Department, Carnegie Mellon University, Pittsburgh, PA 15213, USA; the Mohamed bin Zayed University of Artificial Intelligence, Masdar City, Abu Dhabi, UAE.

J. Cao is with Beijing National Research Center for Information Science and Technology, Tsinghua University, Beijing 100084, China.

Corresponding author: Junwei Cao, email: jcao@tsinghua.edu.cn.

Thus, each agent interacts with a non-stationary environment where the learning process becomes highly unstable.

To address the non-stationary environment during the learning process of decentralized policies, the framework *decentralized actors with centralized critic* (DACC) is widely adopted by previous MARL approaches [16], [22], [23], [24], [25]. The centralized critic of DACC is available to the information of all agents during learning. While, the decentralized actors, i.e., the decentralized policies, are executed using the information only from their corresponding agents. Thus, DACC mitigates the challenge of non-stationary environment during learning. For example, authors in [12] use DACC to learn the cooperative load scheduling of multiple households. However, the advantages of DACC are at the expense of the privacy of agents, since the information of all agents must be shared with the centralized critic during learning.

Another crucial challenge of MARL is known as the *multi-agent credit assignment* problem [26]. In fully cooperative environments, it is intractable for individual agents to deduce their own contributions, since the joint actions of all agents generate only global rewards. Consequently, the agents fail to learn optimal coordinated policies. Sometimes it is possible to manually design individual reward functions for all agents. For example, [10] distributes the total energy costs of a heating, ventilation, and air conditioning (HVAC) system to each appliance by designing specific reward functions. However, this approach is less practical in a general cooperative environment as it is still an open question about how to design the appropriate rewards [16].

C. Contributions

In this work, we intend to minimize the total operation costs of a residential microgrid while preserving the local information of households. This cooperative load scheduling problem is formulated as decentralized partial observable Markov decision process (Dec-POMDP) [27]. Without access to the agents' local information, we propose *decentralized actors with distributed critics* (DADC), a privacy-preserving MARL framework. In this framework, each agent maintains an individual actor and critic, both of which act only on the agent's local observation. The global value function is designed as the sum of the distributed critics. The distributed critics are learnable by backpropagating the gradients from global temporal-difference (TD) updates, which are dependent on the global reward. Put differently, each individual critic is learned implicitly rather than from any reward specific to it. In this way, DADC efficiently addresses the credit assignment problem. We highlight the difference between DADC and the existing actor-critic frameworks in Table I.

To the best of our knowledge, DADC is the first multi-agent actor-critic framework that preserves the local observations of the agents during both training and execution. The contributions of this paper can be summarized as follows.

- We propose DADC, a novel MARL framework to address the cooperative load scheduling problem in a residential microgrid. In contrast to the existing MARL frameworks adopted by most load scheduling schemes [18], [17],

TABLE I
COMPARISON BETWEEN DADC AND THE EXISTING ACTOR-CRITIC FRAMEWORKS.

	CAC	IAC	DACC	DADC
Actor(s)	Centralized	Decentralized	Decentralized	Decentralized
Critic(s)	Centralized	Decentralized	Centralized	Distributed
Credit Assignment			✓	✓
Privacy-Preserving		✓		✓

[8], [9], [10], [11], [12], DADC enables households to perform distributed training and decentralized execution conditioning only on local information, thus preserving the privacy of households.

- DADC can implicitly solve the credit assignment problem without designing the individual reward functions while encouraging all households to cooperatively minimize the total operation costs of the residential microgrid.
- We empirically evaluate the performance of DADC with real-world load data. The results show that DADC outperforms IAC by a large margin and can achieve comparable performance to DACC, a state-of-the-art MARL framework which does not preserve the agents' privacy.

II. PRELIMINARIES

A. Dec-POMDP

An Dec-POMDP [20] can be mathematically described by a tuple $\langle \mathcal{D}, \mathcal{S}, \mathcal{A}, \mathcal{O}, P_o, P_s, R, \gamma \rangle$, where

- \mathcal{D} denotes the set of agents.
- \mathcal{S} denotes the set of global states.
- $\mathcal{A} \equiv \times_{i \in \mathcal{D}} \mathcal{A}_i$ denotes the set of joint actions.
- $\mathcal{O} \equiv \times_{i \in \mathcal{D}} \mathcal{O}_i$ denotes the set of joint observations.
- $P_o : \mathcal{S} \times \mathcal{A} \times \mathcal{O} \mapsto [0, +\infty)$ denotes the joint observation probability distribution.
- $R : \mathcal{S} \times \mathcal{A} \times \mathcal{S} \mapsto \mathbb{R}$ denotes the global reward function.
- $P_s : \mathcal{S} \times \mathcal{A} \times \mathcal{S} \mapsto [0, +\infty)$ denotes the state transition probability distribution.
- γ denotes the discount factor.

At every time step t , each agent i takes an action a_t^i from individual action space \mathcal{A}_i , forming a joint action \mathbf{a}_t which leads to a transition to a new state $\mathbf{s}_{t+1} \sim P_s(\cdot | \mathbf{s}_t, \mathbf{a}_t)$ and a global reward $r_t = R(\mathbf{s}_t, \mathbf{a}_t, \mathbf{s}_{t+1})$. Moreover, the environment emits a joint observation $\mathbf{o}_{t+1} \sim P_o(\cdot | \mathbf{s}_{t+1}, \mathbf{a}_t)$ where each agent i only draws its own observation o_{t+1}^i .

The goal of Dec-POMDP is to learn a joint policy $\pi(\mathbf{a} | \mathbf{o}) : \mathcal{O} \times \mathcal{A} \rightarrow [0, +\infty)$, which maximizes the accumulated discounted global reward $\sum_{t=0}^{T-1} \gamma^t r_t$.

To evaluate the performance of the joint policy π , we define the joint state value function as

$$V^\pi(\mathbf{o}_t) = \mathbb{E}_{\mathbf{s}_{t'} > t, \mathbf{o}_{t'} > t, \mathbf{a}_{t'} \geq t} \left[\sum_{t'=t}^{T-1} \gamma^{t'-t} r_{t'} \mid \mathbf{o}_t \right], \quad (1)$$

where \mathbb{E} is the expectation. The subscript of \mathbb{E} enumerates the variables being integrated over, where the global states, joint observations and actions are sampled sequentially from the dynamics model $P_s(\mathbf{s}_{t+1} | \mathbf{s}_t, \mathbf{a}_t)$, $P_o(\mathbf{o}_{t+1} | \mathbf{s}_{t+1}, \mathbf{a}_t)$ and policy

$\pi(\mathbf{a}_t|\mathbf{o}_t)$, respectively. Similarly, the joint state-action value function is defined as

$$Q^\pi(\mathbf{o}_t, \mathbf{a}_t) = \mathbb{E}_{\mathbf{s}_{t'} > t, \mathbf{o}_{t'} > t, \mathbf{a}_{t'} > t} \left[\sum_{t'=t}^{T-1} \gamma^{t'-t} r_{t'} \mid \mathbf{o}_t, \mathbf{a}_t \right]. \quad (2)$$

The advantage function, widely used by policy-based DRL, is

$$A^\pi(\mathbf{o}_t, \mathbf{a}_t) = Q^\pi(\mathbf{o}_t, \mathbf{a}_t) - V^\pi(\mathbf{o}_t), \quad (3)$$

which measures whether the action \mathbf{a}_t is better than the default behaviour of policy π .

III. PROBLEM FORMULATION

A. System Description

We consider an isolated residential microgrid with distributed generators (DGs). The residential microgrid provides power to a set $\mathcal{D} = \{1, \dots, n\}$ of n households. Without loss of generality, each household is assumed to be equipped with base loads, one EV and one air conditioner (AC), as shown in Fig. 1. Moreover, there exists one home energy management system (HEMS) for each household to schedule the controllable appliances including AC and EV. For privacy-preserving purpose, each HEMS can only access the common information from DGs and its own local information. We consider this problem over the horizon T with each time step Δt , i.e., $t \in \mathcal{T} = \{0, 1, \dots, T-1\}$.

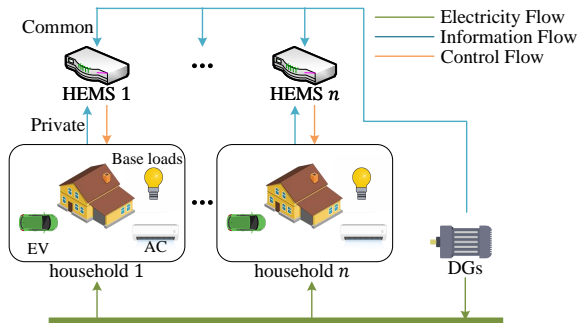


Fig. 1. The overview of the considered residential microgrid. The DGs supply electricity to households. The HEMSs of households take the public information from DGs and the private observations from local households as input, and generate control signals for the local load scheduling.

B. System Model

The ACs can be dynamically adjusted to maintain thermal comfort of the occupants in the corresponding households. The dynamics of indoor temperature in household i can be presented as follows,

$$T_{t+1}^i = F_i^{AC}(T_t^i, T_{i,t}^{out}, P_{i,t}^{AC}, \varrho_t^i), \quad (4)$$

where $F_i^{AC}(\cdot)$ denotes the transition function of indoor temperature with respect to four variables, i.e., current indoor temperature, outdoor temperature, AC power, and disturbance at time step t . Normally, it is intractable to obtain accurate thermal dynamics models. Therefore, we assume that the

explicit form of function $F_i^{AC}(\cdot)$ is hard to be captured. The working power of ACs can be continuously adjusted within a range,

$$0 \leq P_{i,t}^{AC} \leq P_{i,max}^{AC}, \quad (5)$$

where $P_{i,max}^{AC}$ denotes the maximum working power of the AC in household i . To ensure the thermal comfort of occupants, the following indoor temperature constraint should be satisfied,

$$T_{min}^i \leq T_t^i \leq T_{max}^i, \quad (6)$$

where T_{min}^i, T_{max}^i denote the desirable minimum and maximum indoor temperature in household i , respectively.

It is assumed that EVs can be charged or discharged during parking time. The dynamics of EV battery energy in household i can be represented as follows,

$$E_{t+1}^i = \begin{cases} E_{init}^i, & \text{if } t+1 = t_a^i, \\ E_t^i + \eta_i^c P_{i,t}^{EV} \Delta t, & \text{if } t_a^i \leq t < t_d^i \text{ and } P_{i,t}^{EV} \geq 0, \\ E_t^i + P_{i,t}^{EV} \Delta t / \eta_i^d, & \text{if } t_a^i \leq t < t_d^i \text{ and } P_{i,t}^{EV} < 0, \\ 0, & \text{otherwise.} \end{cases} \quad (7)$$

In (7), the variables E_t^i and $P_{i,t}^{EV}$ are the battery energy and the charging/discharging power of the EV in household i at time step t , respectively. The parameters $E_{init}^i, \eta_i^c, \eta_i^d, t_a^i$ and t_d^i are the initial battery energy, the charging and discharging efficiency coefficients, the arrival time and departure time of the EV in household i , respectively. The target EV battery energy should be satisfied at the departure time of the EV,

$$E_t^i|_{t=t_d^i} \geq E_{targ}^i, \quad (8)$$

where E_{targ}^i denotes the target battery energy of the EV in household i . Moreover, the charging/discharging power and the battery energy of the EV must be maintained within a range,

$$-P_{i,max}^{EV} \leq P_{i,t}^{EV} \leq P_{i,max}^{EV}, E_{min}^i \leq E_t^i \leq E_{max}^i, \quad (9)$$

where $P_{i,max}^{EV}, E_{min}^i$ and E_{max}^i represent the maximum charging/discharging power, the minimum and maximum battery energy of the EV in household i .

At each time step t , DGs are automatically adjusted to maintain the power balance in the whole microgrid,

$$P_t^{DG} = \sum_{i \in \mathcal{D}} P_{i,t}^{BL} + P_{i,t}^{AC} + P_{i,t}^{EV}, \quad (10)$$

where $P_{i,t}^{BL}$ denotes the power of base loads in household i at time step t .

C. Objective Function

The total operation cost of the microgrid can be divided into two parts, the generation cost of DGs and the adjustment cost of DGs. The former is determined by the output power of DGs. The latter depends on the fluctuation of the output power of DGs because the frequent power adjustment would degrade the service life of DGs. Thus, the total cost at time step t can be presented as follows.

$$C_t = G_1(P_t^{DG}) + G_2(P_t^{DG} - P_{t-1}^{DG}), \quad (11)$$

where $G_1(\cdot)$ is the generation cost function of DGs with respect to current output power of DGs, and $G_2(\cdot)$ is the adjustment cost function of DGs with respect to the difference between the output power of DGs at current and last time step. It is notable that the functions $G_1(\cdot)$ and $G_2(\cdot)$ can be non-linear, thus the individual cost functions specific to households are not generally available.

Based on the above-mentioned models and objective function, a stochastic optimization problem with the aim of minimizing the long-term microgrid operation cost can be formulated as follows,

$$\begin{aligned} \text{(P1)} \quad & \min_{P_{i,t}^{AC}, P_{i,t}^{EV}} \mathbb{E} \left[\sum_{t \in \mathcal{T}} C_t \right] \\ & \text{s.t.} \quad (4) - (11) \end{aligned} \quad (12)$$

D. Dec-POMDP Formulation

In this subsection, we formulate the cooperative load scheduling problem following Dec-POMDP. The agents in Dec-POMDP are specified as the HEMSs in the microgrid. Since the model-free MARL does not rely on the global state and the state transition probability distribution, we focus on three components, i.e. the observations, the actions, and the global reward function.

1) *Observations*: To facilitate the cooperative scheduling of all households, the power of DGs is viewed as common information and provided to each HEMS. The observation of HEMS i ($i \in \mathcal{D}$) is defined as

$$o_t^i = [t, P_t^{DG}, P_{i,t}^{BL}, P_{i,t}^{PV}, T_{i,t}^{out}, T_t^i, E_t^i, E_{targ}^i, t_d^i], \quad (13)$$

The last seven components in 13 are local information of household i which should be preserved.

2) *Actions*: To facilitate the training of MADRL, we unify the continuous action spaces to $[-1, 1]$ by introducing control signals for ACs and EVs, respectively. The relationship between the control signals decided by the HEMS and the working power executed by home appliances is presented as follows.

To guarantee the thermal comfort of the occupants and satisfy the indoor temperature constraint (6), the following scheme is designed,

$$P_{i,t}^{AC} = P_{i,max}^{AC} \begin{cases} 1, & \text{if } T_{i,t} \geq T_i^{max}, \\ 0, & \text{if } T_{i,t} \leq T_i^{min}, \\ 0.5(u_{i,t}^{AC} + 1), & \text{otherwise.} \end{cases} \quad (14)$$

Under this scheme, ACs would take corresponding mode to ameliorate the thermal condition: run at the maximum power if current indoor temperature is above desirable maximum temperature; turn-off if current indoor temperature is below the desirable minimum temperature.

Considering that the EV charging task (8) should be completed before the departure time, the following inequality must be checked for each time step $t_a^i \leq t < t_d^i$,

$$E_t^i + \eta_i^c P_{i,max}^{EV} (t_d^i - t) \Delta t \geq E_{targ}^i, \quad (15)$$

where the left part indicates the EV battery energy at departure time if the EV is charged at maximum charging power during remaining charging time. Once inequality (15) is not satisfied, the EV must be charged at maximum power. Therefore, the following EV charging scheme during the charging time is formulated,

$$P_{i,t}^{EV} = P_{i,max}^{EV} \begin{cases} 1, & \text{if (15) not satisfied,} \\ \max\{0, u_{i,t}^{EV}\}, & \text{else if } E_t^i \leq E_{min}^i, \\ \min\{0, u_{i,t}^{EV}\}, & \text{else if } E_t^i \geq E_{max}^i, \\ u_{i,t}^{EV}, & \text{otherwise.} \end{cases} \quad (16)$$

The 2nd and 3rd conditions in (16) are designed to ensure that the battery energy of EV in household i satisfies the constraint (9).

In this sense, the individual action of HEMS i at time step t is presented as

$$a_t^i = [u_{i,t}^{AC}, u_{i,t}^{EV}] \in [-1, 1]^2, i \in \mathcal{D}. \quad (17)$$

And the joint action formed by individual actions of all HEMSs at time step t is

$$\mathbf{a}_t = [a_t^1, \dots, a_t^n] \in [-1, 1]^{2n}. \quad (18)$$

3) *Reward*: The load scheduling problem intends to minimize the total operation cost, while the goal of Dec-POMDP is to maximize the accumulated reward. Therefore, we define the immediate reward taking joint action \mathbf{a}_t in state s_t as the negative cost of DGs,

$$r_t = -C_t. \quad (19)$$

IV. PRIVACY-PRESERVING ACTOR-CRITIC FRAMEWORK

As stated in Sec. 1, confronted with the formulated Dec-POMDP, the existing actor-critic frameworks fail to address the credit assignment problem and preserve the user privacy simultaneously. In this section, we first propose DADC, a privacy-preserving actor-critic framework which allows agents to preserve their local observations during both training and execution. Then, we elaborate the distributed training for DADC with the on-policy and off-policy algorithms, respectively. Finally, we present the fully decentralized execution with learned policies.

A. Architecture

DADC maintains the structure of decentralized actors and distributed critics. The critics can be used to estimate both the state value function and action-state value function. For demonstration purposes, we intuitively present the structure of DADC with the critics approximating the state value function in Fig. 2. We elaborate this structure as follows.

1) *Decentralized Actors*: Each agent learns a stochastic policy $\pi^i : \mathcal{O}_i \times \mathcal{A}_i \rightarrow [0, +\infty)$, which is parameterized by θ^i and maps each agent's observation to a probability distribution over its action space. Note that the policy π^i is only conditioned on the local observation o^i . Then, the joint

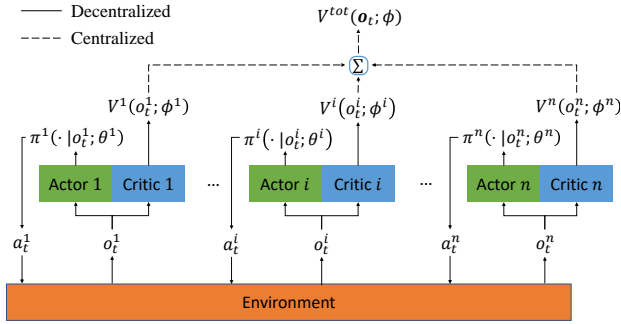


Fig. 2. The framework of DADC. Each agent’s actor generates individual policy π^i only using its local observation o_t^i , and then the individual action a_t^i is sampled according to policy π^i . Each agent’s critic estimates the individual value function only using its local observation o_t^i , and then the global value function is computed with the sum of individual value functions.

policy π is constructed by the decentralized policies $\{\pi^i\}_{i=1}^n$, i.e.,

$$\pi(\mathbf{a}_t | \mathbf{o}_t; \theta) \triangleq \prod_{i=1}^n \pi^i(a_t^i | o_t^i; \theta^i), \quad (20)$$

where $\theta = \{\theta^i\}_{i=1}^n$.

2) *Distributed Critics*: DACC adopted by existing cooperative multi-agent actor-critic approaches has a centralized critic to approximate the global value function of the joint policy, which requires the global state including all agents’ local observations, although the decentralized execution is allowed after training. For privacy-preserving purposes, the proposed DADC approximates the global value function by the additive decomposition form,

$$V^\pi(\mathbf{o}_t) \approx V^{tot}(\mathbf{o}_t; \phi) \triangleq \sum_{i=1}^n V^i(o_t^i; \phi^i), \quad (21)$$

where $V^i(\cdot; \phi^i) : \mathcal{O}_i \rightarrow \mathcal{R}$ is the individual critic parameterized by ϕ^i , and $\phi = \{\phi^i\}_{i=1}^n$. In this way, the calculation of the global value function only requires to collect the outputs of individual critics, and does not rely on the access to all agents’ local observations. Moreover, this decomposed form enables the agent to implicitly learn credit assignment with the end-to-end training.

The individual actors and critics are shown in Fig. 3. The policy of each agent is represented as the combination of gate recurrent unit (GRU) [28] and multilayer perceptrons (MLPs) [29]. The MLPs are feedforward neural networks with powerful representation capability due to the multi-layered structure. The GRU module, a gating mechanism in recurrent neural networks (RNNs) [30], use the hidden state $h_{t-1, \pi}^i$ to memory the information before the step t , which enables the agent to alleviate the severe problem of partial observability. Therefore, with the integration of a GRU module and MLPs, the individual actor network has the potential to generate a good policy given limit observation. Similar to the inner structure of individual actor network, the individual critic network is also concatenated by a GRU module and two MLPs.

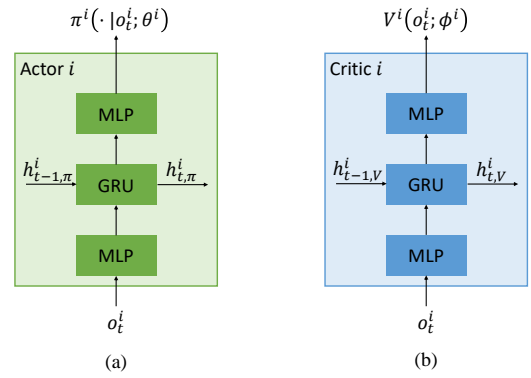


Fig. 3. (a) Individual actor network. This network take the local observation o_t^i and the hidden state at last time step $h_{t-1, \pi}^i$ as input, and generates the probability distribution over the individual action space. (b) Individual critic network. This network take the local observation o_t^i and the hidden state at last time step $h_{t-1, V}^i$ as input, and generates the individual value function.

The DADC enables the agents to preserve their local observations during the calculation of both decentralized policies and global value function.

B. Distributed Training: On-Policy

DADC can be trained by both the on-policy and off-policy algorithms in a distributed manner. In this subsection, we present the on-policy learning for DADC. For demonstration purposes, we take the PPO algorithm [31] as an example and adapt the single-agent PPO to the multi-agent and privacy-preserving settings.

1) *Algorithm*: Normally, the on-policy RL approaches compute an estimator of the policy gradient by differentiating the objective $\mathbb{E}_t[\pi(\mathbf{a}_t | \mathbf{o}_t; \theta) \Psi_t]$. The choice $\Psi_t = A^\pi(\mathbf{o}_t, \mathbf{a}_t)$ yields almost the lowest possible variance [32]. In practice, the advantage function $A^\pi(\mathbf{o}_t, \mathbf{a}_t)$ is not known, and we estimate it by the general advantage estimation (GAE) method [33] as follows,

$$\hat{A}_t = \sum_{t'=t}^{T-1} (\gamma\lambda)^{t'-t} (-V^{tot}(\mathbf{o}_{t'}; \phi) + r_{t'} + \gamma V^{tot}(\mathbf{o}_{t'+1}, \phi)),$$

where \hat{A}_t is the estimate to $A^\pi(\mathbf{o}_t, \mathbf{a}_t)$, and the parameter λ is used to control the trade-off between variance and bias of the estimate.

To improve the sample efficiency, we intend to update parameters of actors and critics several times during one sample. Except the first update, the networks used for update is different from the networks used for sampling. To avoid the excessively large policy update during one sample, the following clipped surrogate objective is employed,

$$\mathcal{L}_a = \mathbb{E}_t \left[\min \left(w_t(\theta) \hat{A}_t, \text{clip} \left(w_t(\theta), 1 - \epsilon, 1 + \epsilon \right) \hat{A}_t \right) \right],$$

where ϵ is a hyperparameter, and the joint probability ratio $w_t(\theta)$ is defined as

$$w_t(\theta) = \prod_{i=1}^n w_t^i(\theta^i) = \prod_{i=1}^n \frac{\pi^i(a_t^i | o_t^i; \theta^i)}{\pi^i(a_t^i | o_t^i; \theta_{old}^i)}. \quad (22)$$

Here, θ_{old} is policy parameters of agent i the before the update. With the advantage estimated by GAE method, the reward-to-go can be presented as $\hat{R}_t = \hat{A}_t + V^{tot}(\mathbf{o}_t; \phi)$, and the critics are updated by minimizing the loss

$$\mathcal{L}_c = \mathbb{E}_t \left[\left(V^{tot}(\mathbf{o}_t; \phi) - \hat{R}_t \right)^2 \right]. \quad (23)$$

In this way, each individual critic $V^i(\cdot; \phi^i)$ is learned by back-propagating the gradients from global TD updates, which is dependent on the joint global reward. Put differently, $V^i(\cdot; \phi^i)$ is learned implicitly rather than from any reward specific to agent i .

2) *Workflow*: The on-policy training process is detailed in Algo. 1. Overall, the training during one iteration can be divided into three parts, i.e., interacting with the environment, calculating the advantage and return-to-go, performing parameter updates.

The first part, shown in lines 4-10 of Algo. 1, is conducted by agents in a fully decentralized manner. At each time step t , each agent i interacts with the environment by independently selecting and executing its own action. The only information uploaded to centralized trainer is the value function calculated by each agent, which does not reveal the user privacy. Note that above-mentioned operations are conducted concurrently by agents.

The second part is performed by the centralized trainer. As shown in line 14, the calculation for centralized critic only relies on the individual values uploaded by agents, rather than the global states including all agents' observations. The calculation for advantages and returns at time step t uses advantages and returns at time step $t + 1$, which is oriented backward in time.

The third part is executed alternately by agents and the centralized trainer. First, each agent calculates and uploads the individual ratio and value function in parallel. Then, the centralized trainer uses the collected information to calculate the global actor loss and critic loss, whose partial derivatives with respect to collected information are distributed to corresponding agents. The agents uses the received partial derivatives to calculate the gradients of global losses to local parameters. Finally, the accumulated gradients are used for the update of individual actors and critics. Owing to $\partial \mathcal{L}_a / \partial w_t^i$ and $\partial \mathcal{L}_c / \partial v_t^i$ as intermediate results, the gradients of global losses to local parameters can be jointly calculated without exposing local observations to centralized trainer.

C. Distributed Training: Off-Policy

DADC also supports the off-policy training in which *replay buffer* is used to store the experience [34]. For privacy purposes, we store the joint experience $(\mathbf{o}_t, \mathbf{a}_t, r_t, \mathbf{o}_{t+1})$ in distributed buffers owned by agents, instead of a centralized buffer. To be specific, the buffer of each agent is employed to memory its local experience $(o_t^i, a_t^i, r_t, o_{t+1}^i)$. To sample the joint experience from the distributed buffers correctly, all agents should simultaneously sample their local experiences according to the same sampling index. We denote \mathcal{B}^i as the replay buffer of agent i , and all distributed buffers form the joint replay buffer \mathcal{B}^{tot} .

Algorithm 1 Distributed Training with PPO

```

1: Initialize  $\theta^i$  and  $\phi^i$  for each agent
2: for  $episode = 1$  to  $episode_{max}$  do
3:   for  $t = 0$  to  $T - 1$  do  $\triangleright$  Interact with environment
4:     for agent  $i = 1$  to  $n$  do  $\triangleright$  Decentralized
5:       Generate policy  $\pi^i(\cdot | o_t^i; \theta^i)$ .
6:       Sample action  $a_t^i \sim \pi^i(\cdot | o_t^i; \theta^i)$ .
7:       Execute action  $a_t^i$  and receive  $o_{t+1}^i, r_t$ .
8:        $p_{t,old}^i \leftarrow \pi^i(a_t^i | o_t^i; \theta^i)$ ,  $v_t^i \leftarrow V^i(o_t^i; \phi^i)$ .
9:       Upload  $v_t^i$ .
10:   %Compute advantage and return-to-go.  $\triangleright$  Centralized
11:    $\hat{A}_T \leftarrow 0$ ,  $V_T^{tot} \leftarrow 0$ 
12:   for  $t = T - 1$  to  $0$  do
13:      $V_t^{tot} \leftarrow \sum_{i=1}^n v_t^i$ 
14:      $\hat{R}_t \leftarrow \gamma \lambda \hat{A}_{t+1} + r_t + \gamma V_{t+1}^{tot}$ 
15:      $\hat{A}_t \leftarrow \hat{R}_t - V_t^{tot}$ 
16:   for  $k = 1$  to  $K$  do  $\triangleright$  Parameter update
17:     for  $t = 0$  to  $T - 1$  do
18:       for agent  $i = 1$  to  $n$  do  $\triangleright$  Decentralized
19:          $w_t^i \leftarrow \pi^i(a_t^i | o_t^i; \theta^i) / p_{t,old}^i$ ,  $v_t^i \leftarrow V^i(o_t^i; \phi^i)$ 
20:         Upload  $v_t^i$  and  $w_t^i$ .
21:        $w_t \leftarrow \prod_{i=1}^n w_t^i$   $\triangleright$  Centralized
22:        $\mathcal{L}_a \leftarrow \min \left( w_t \hat{A}_t, \text{clip}(w_t, 1 - \epsilon, 1 + \epsilon) \hat{A}_t \right)$ 
23:        $\mathcal{L}_c \leftarrow \left( \sum_{i=1}^n v_t^i - \hat{R}_t \right)^2$ 
24:       Send  $\partial \mathcal{L}_a / \partial w_t^i$  and  $\partial \mathcal{L}_c / \partial v_t^i$  to each agent.
25:       for agent  $i = 1$  to  $n$  do  $\triangleright$  Decentralized
26:          $g_a^i \leftarrow g_a^i + \partial \mathcal{L}_a / \partial w_t^i \cdot \partial w_t^i / \partial \theta_t^i$ 
27:          $g_c^i \leftarrow g_c^i + \partial \mathcal{L}_c / \partial v_t^i \cdot \partial v_t^i / \partial \phi_t^i$ 
28:       for agent  $i = 1$  to  $n$  do  $\triangleright$  Decentralized
29:         Update  $\theta^i$  with gradient  $g_a^i$ .
30:         Update  $\phi^i$  with gradient  $g_c^i$ .

```

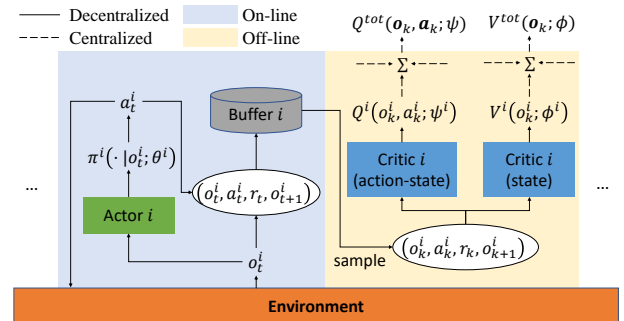


Fig. 4. Off-policy training for DADC. Left: Each agent interacts with the environment and stores the local experience in its own replay buffer. Right: The local experience is sampled from the individual buffer and used to compute the individual value functions; then the global value functions are computed with the sum of individual value functions.

1) *Algorithm*: We demonstrate the training for DADC with a specific off-policy RL algorithm, i.e., SAC [35]. The SAC approach aims to learn three functions $\pi(\cdot|\cdot; \theta)$, $V^{tot}(\cdot; \phi)$, $Q^{tot}(\cdot, \cdot; \psi)$ by minimizing the following loss functions:

$$\mathcal{L}_Q = \mathbb{E}_{(\mathbf{o}_k, \mathbf{a}_k, r_k, \mathbf{o}_{k+1}) \sim \mathcal{B}^{tot}} \left[\left(Q^{tot}(\mathbf{o}_k, \mathbf{a}_k; \psi) - r_k - \gamma V^{tot}(\mathbf{o}_{k+1}; \phi) \right)^2 \right], \quad (24)$$

$$\mathcal{L}_V = \mathbb{E}_{(\mathbf{o}_k, \mathbf{a}_k, r_k, \mathbf{o}_{k+1}) \sim \mathcal{B}^{tot}} \left[\left(V^{tot}(\mathbf{o}_k; \phi) - \hat{V}_k \right)^2 \right], \quad (25)$$

$$\mathcal{L}_\pi = \mathbb{E}_{(\mathbf{o}_k, \mathbf{a}_k, r_k, \mathbf{o}_{k+1}) \sim \mathcal{B}^{tot}} \left[\log \pi(\mathbf{a}_k | \mathbf{o}_k; \theta) - Q^{tot}(\mathbf{o}_k, \mathbf{a}_k; \psi) \right], \quad (26)$$

where

$$\hat{V}_k = \mathbb{E}_{\mathbf{a}_k \sim \pi(\cdot | \mathbf{o}_k; \theta)} \left[Q^{tot}(\mathbf{o}_k, \mathbf{a}_k; \psi) - \log \pi(\mathbf{a}_k | \mathbf{o}_k; \theta) \right].$$

2) *Workflow*: The off-policy training process is detailed in Algo. 2. Overall, the training can be divided into two parts, i.e., the on-line interaction with the environment, and the off-line parameter update. Next, we focus on the difference between on-policy and off-policy training.

The first part is shown in lines 3-8 of Algo. 2. At each time step t , after the decentralized interaction with the environment, the agent's experience is stored locally in the individual buffer \mathcal{B}_i .

The second part is shown in lines 9-25 of Algo. 2. First, the centralized trainer determine the index of samples, and all agents draw their local experiences from their buffers according to the sampling index simultaneously. Then, each agent generates and uploads the individual probability and value functions for the centralized computation of the global actor loss and critic loss.

D. Decentralized Execution

With the agents' trained policies, the fully decentralized execution can be performed, as shown in Algo. 3. Note that there is no any communication between agents during execution.

V. EXPERIMENTS

In this section, we conduct the simulation experiments and report the simulation results. First, the simulation experiment setup and algorithmic settings are presented. Second, we compare our DADC with prior actor-critic frameworks using the on-policy PPO algorithms. Third, we investigate the sample efficiency and training efficiency of the on-policy and off-policy training for DADC.

A. Experiment Setup and Implementation

1) *Environment*: The simulation environment is builed with OpenAI Gym [36], consisting of 10 heterogeneous households. The dynamics functions, cost functions and important parameters of households are provided in Appendix. We consider the energy management problem during one day. We use a time step of 15 minutes, such that the time horizon T is 96. The real-world power data and temperature data are employed to model the power of basic loads and outdoor temperature, which are available from Pecan Street Database[37] and NOAA[38].

Algorithm 2 Distributed Training with SAC

```

1: Initialize  $\theta^i$ ,  $\phi^i$ , and  $\psi^i$  for each agent
2: for  $episode = 1$  to  $episode_{max}$  do
3:   for  $t = 0$  to  $T - 1$  do ▷ On-line
4:     for agent  $i = 1$  to  $n$  do ▷ Decentralized
5:       Generate policy  $\pi^i(\cdot | o_t^i; \theta^i)$ .
6:       Sample action  $a_t^i \sim \pi^i(\cdot | o_t^i; \theta^i)$ .
7:       Execute action  $a_t^i$  and receive  $o_{t+1}^i, r_t$ .
8:       Store  $(o_t^i, a_t^i, r_t, o_{t+1}^i)$  in  $\mathcal{B}_i$ .
9:   Determine the index of  $K$  samples. ▷ Centralized
10:  for agent  $i = 1$  to  $n$  do ▷ Decentralized
11:    Sample  $\{(o_k^i, a_k^i, r_k, o_{k+1}^i)\}_{k=1}^K$  from  $\mathcal{B}_i$  according
    to the index.
12:  for  $k = 1$  to  $K$  do ▷ Off-line
13:    for agent  $i = 1$  to  $n$  do ▷ Decentralized
14:       $p^i \leftarrow \pi^i(a_k^i | o_k^i; \theta^i), v^i \leftarrow V^i(o_k^i; \phi^i), q^i \leftarrow$ 
       $Q^i(o_k^i, a_k^i; \psi^i)$ 
15:      Upload  $p^i, v^i, q^i$ .
16:       $p \leftarrow \prod_{i=1}^n p^i$  ▷ Centralized
17:       $v^{tot} \leftarrow \sum_{i=1}^n v^i, q^{tot} \leftarrow \sum_{i=1}^n q^i$ 
18:      Compute  $\mathcal{L}_\pi, \mathcal{L}_V, \mathcal{L}_Q$  according to (24)-(26).
19:      Send  $\partial \mathcal{L}_\pi / \partial p^i, \partial \mathcal{L}_Q / \partial q^i, \partial \mathcal{L}_V / \partial v^i$  to each agent.
20:      for agent  $i = 1$  to  $n$  do ▷ Decentralized
21:         $g_\pi^i \leftarrow g_\pi^i + \partial \mathcal{L}_\pi / \partial p^i \cdot \partial p^i / \partial \theta^i$ 
22:         $g_V^i \leftarrow g_V^i + \partial \mathcal{L}_V / \partial v^i \cdot \partial v^i / \partial \phi^i$ 
23:         $g_Q^i \leftarrow g_Q^i + \partial \mathcal{L}_Q / \partial q^i \cdot \partial q^i / \partial \psi^i$ 
24:      for agent  $i = 1$  to  $n$  do ▷ Decentralized
25:        Update  $\theta^i, \phi^i, \psi^i$  with gradient  $g_\pi^i, g_V^i, g_Q^i$ .
```

Algorithm 3 Decentralized Execution

```

Each agent  $i$  loads the parameter  $\theta^i$  for the actor in parallel.
Each agent  $i$  receives initial observation  $o_0^i$  in parallel.
for  $t = 0$  to  $T - 1$  do
  for agent  $i = 1$  to  $n$  do
    Generate policy  $\pi^i(\cdot | o_t^i; \theta^i)$ .
    Sample action  $a_t^i$  according to  $\pi^i(\cdot | o_t^i; \theta^i)$ .
    Execute action  $a_t^i$  and observe  $o_{t+1}^i$ .
```

2) *Network Architecture*: The individual critic networks share the same structure, consisting of three components, as shown in Fig. 2, a fully-connected MLP with two layers of 128 units and tanh nonlinearities, a GRU layer with 64 units, and a fully-connected MLP with one hidden layer of 128 units and one output layer of 1 units.

To represent the stochastic policy, we use the Gaussian distribution $\mathcal{N}(\mu, \sigma^2)$ in this work. Therefore, the individual actor networks have one tanh output for the mean μ and another sigmoid output for the variance σ^2 . The non-output layers of individual actor networks share the same structure with the individual critic networks.

3) *Shared Hyperparameters*: We optimize the actor and critic networks using Adam [39] with the learning rate of 1×10^{-4} and 3×10^{-4} , respectively. The discount factor γ is set to be 0.99. The network weights are updated every 120 environment steps with the batch size of 120. We run 10

parallel environments to improve the training efficiency. The case studies are conducted on a server with an 8-core AMD Ryzen 7 3700X processor and one single GeForce RTX 2080 GPU.

B. Main Results

First, we compare DADC with other actor-critic frameworks on the formulated cooperative load scheduling problem. Baseline comparison frameworks include IAC and DACC, and we train the networks of all frameworks with on-policy PPO algorithms. For PPO, the GAE parameter is set be 0.95, and the network weights are updated 3 times during one sample [31].

We train the proposed framework for six times with different random seeds. In order to evaluate the performance during training, we adopt the following evaluation procedure: for each trial of a framework, we pause the training every 1000 episodes and run 10 independent episodes with each agent performing decentralized action selection. The sum of reward during an episode is referred to as the *episode reward*.

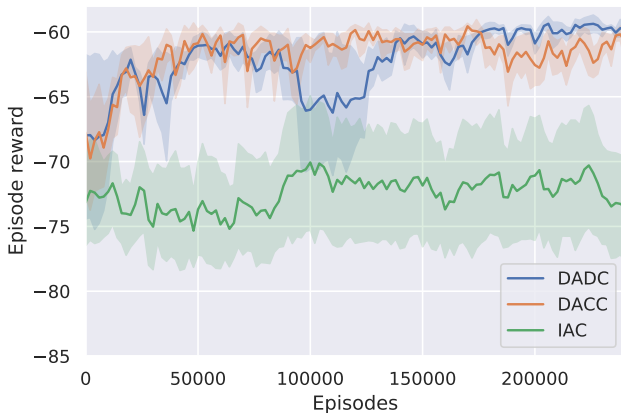


Fig. 5. Training curves of DADC and other frameworks. The solid curves corresponds to the mean and the shaded region to the minimum and maximum episode rewards over the all trials.

We can observe from Fig. 5 that IAC fails to learn stable policies and result in poor performance. This highly unstable training can be attributed to the non-stationarity in the environment of IAC. In contrast, benefiting the centralized critic, DACC is able to more stably learn the coordinated behaviours across all agents. Furthermore, DADC can learn stable policies with the negative episode reward greater than -60. Note that DADC preserves the agents' local information while DACC fails. Therefore, Fig. 5 shows the superior performance of DADC over other actor-critic frameworks.

C. Effect of Implicit Credit Assignment

As stated in Section I-B, DACC is able to implicitly learn credit assignment across agents. To demonstrate this point, we plot the value loss for critic networks in Fig. 6. We can observe the independent critic networks of IAC have the maximum bias of estimate, because the fully decentralized agent in IAC cannot capture the other agents changing their behaviour during training.

Due to the centralized critic, the value loss of DACC is relatively smaller than that of IAC. However, the estimate for value function is highly unstable during training. This can be explained as follows. The centralized critic of DACC takes the observations of all agents, thus it cannot rapidly adapts the change of global reward when one specific agent changes the behaviour.

In contrast, all agents cooperatively estimates the global value function with distributed critic networks in DADC. The individual value function can be learned with the end-to-end training. Therefore, we can observe from Fig. 6 that the value loss for DADC is much smaller than that for IAC and DACC. This demonstrates the effect of implicit credit assignment in DADC.

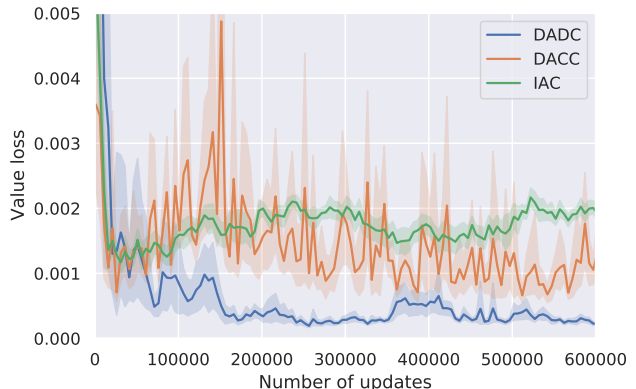


Fig. 6. The value loss for critic networks. DADC achieve the lowest estimation bias for the value function.

D. Effect of Load Scheduling

Next, we specify the control effects of DADC on the cooperative load scheduling problem. After training, we test the policies with best evaluation performance during training. The test results shown in Table II demonstrate that the average cost of DADC is reduced by 11% than that of IAC. Especially, the adjustment cost is reduced by more than 50%.

TABLE II
TEST PERFORMANCE FOR DADC AND IAC

Metrics	DADC	IAC
Average Total Cost	58.201 \pm 0.953	65.390 \pm 1.198
Average Generation Cost	55.790 \pm 1.038	60.535 \pm 1.502
Average Adjustment Cost	2.411 \pm 0.334	4.855 \pm 0.776

To present the control effects for ACs, we plot the indoor temperature curves associated with one AC during one day in Fig. 7. We can observe that both two framework can control the indoor temperature within the constraint. However, the indoor temperature with DADC is closer to the upper temperature constraint when outdoor temperature is high, which can save energy and reduce cost compared with IAC. Moreover, we can see that the indoor temperature curve with DADC is relatively smooth, indicating fewer adjustments to the AC compared with IAC.

To demonstrate the overall load scheduling, the power of base load, the power of DGs, the total charging/discharging

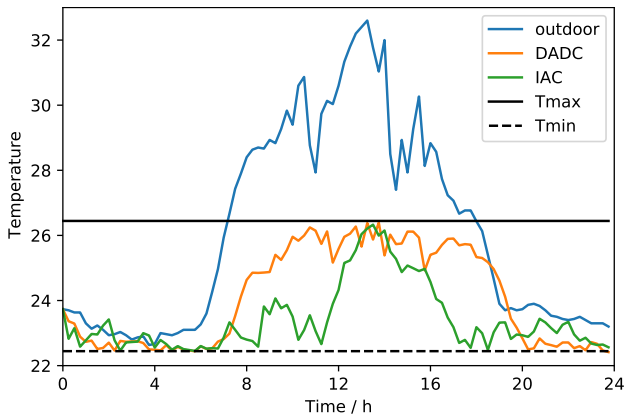


Fig. 7. Indoor temperature. The black solid and dashed lines denote the desirable maximum and minimum indoor temperature, respectively. The orange and green lines denote the indoor temperature curves during one day controlled by decentralized policies with DADC and IAC, respectively.

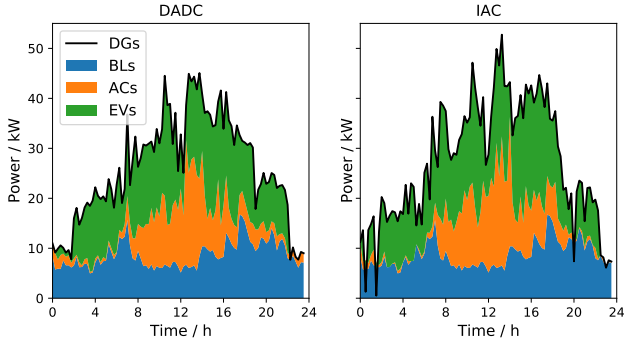


Fig. 8. Load scheduling. The blue, orange and green area denote the power of base load, the total power of ACs and the total charging power, respectively.

power of EVs and the total working power of ACs are presented in Fig. 8. We can see that with DADC, the adjustments for the output power of DGs is relatively flat and the peak power of DGs is smaller than that with IAC. In this sense, DADC is able to learn the decentralized policies such that agents can cooperatively schedule load and reduce the global cost. While, IAC fails to learn such policies due to the fully independent actor-critic structure.

E. Comparison of On-Policy and Off-Policy Training

DADC can be trained with both the on-policy and off-policy algorithms. To investigate the effects of on-policy and off-policy training, we compare DADC with on-policy PPO algorithm to DADC with off-policy SAC algorithm. For SAC, the replay buffer size is set to be 1×10^5 , and the network weights are updated 60 times every 120 environment steps.

We can observe from Fig. 9 that the off-policy training for DADC converges with much fewer interactions. Fig. 10 demonstrates that the on-policy training for DADC learns the policies with higher performance while the off-policy training converges to a lower local optima. Therefore, the off-policy training outperforms the on-policy training in data efficiency, while the on-policy training outperforms the off-policy training in learning efficiency.

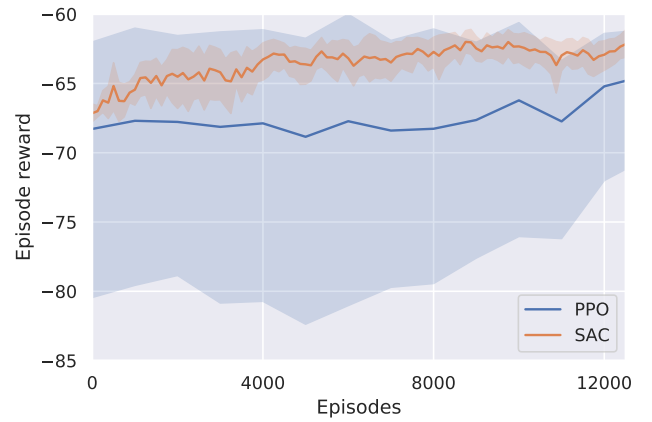


Fig. 9. Performances with respect to the number of episodes. The training with off-policy SAC rapidly converge with lower variance, while the training with on-policy PPO relies on massive interactions.



Fig. 10. Performances with respect to the number of updates. The training with off-policy SAC is more stable, but eventually only learns the locally optimal policies. While, the training with on-policy PPO can learn the policies with better performance.

VI. CONCLUSION

In this paper, a novel multi-agent actor-critic framework, DADC, is proposed to address the privacy-preserving cooperative load scheduling problem in a residential microgrid. The structure of decentralized actors and distributed critics can cope with the multi-agent credit assignment and privacy issues of households simultaneously. Compared with the independent actor-critic framework, DADC can implicitly address the credit assignment problem and stabilize the learning process. Compared with the state-of-the-art MARL framework, DADC can achieve comparable performance while preserving the agents' local information.

APPENDIX

The transition functions and cost functions used for simulation are specified as follows.

$$F_i^{AC}(T, T^{out}, P, \varrho) = T + a^i(T^{out} - T) - b^i P + \varrho, (27)$$

where a^i and b^i are the coefficients associated with the thermal characteristics of corresponding room and AC, and ϱ follows the uniform distribution $\mathcal{U}[-0.1, 0.1]$.

TABLE III
PARAMETERS OF HOUSEHOLDS

i	T_{min}^i	T_{max}^i	$P_{i,max}^{AC}$	a^i	b^i	$P_{i,max}^{EV}$	E_{max}^i
1	22.0	26.0	3.0	0.2	0.667	6.67	40
2	22.2	26.2	3.1	0.2	0.645	7.00	42
3	22.4	26.4	3.2	0.2	0.625	7.33	44
4	22.6	26.6	3.3	0.2	0.606	7.67	46
5	22.8	26.8	3.4	0.2	0.588	8.00	48
6	23.0	26.0	3.5	0.2	0.571	8.33	50
7	23.2	27.2	3.6	0.2	0.555	8.67	52
8	23.4	27.4	3.7	0.2	0.541	9.00	54
9	23.6	27.6	3.8	0.2	0.526	9.33	56
10	23.8	27.8	3.9	0.2	0.513	9.67	58

The cost functions of DGs are specified as

$$G_1(P) = \lambda_1^{DG} P + \lambda_2^{DG} P^2, \quad (28)$$

$$G_2(P_t, P_{t-1}) = \lambda_3^{DG} |P_t - P_{t-1}|. \quad (29)$$

where $\lambda_1, \lambda_2, \lambda_3$ denote the cost coefficients of DGs, and are selected as 0.5, 0.0125 and 0.1, respectively.

The weights of actor networks and critic networks in IAC are updated by minimizing the following loss functions, respectively.

$$\mathcal{L}_a^i = \mathbb{E}_t \left[\min \left(w_t^i(\theta^i) \hat{A}_t^i, \text{clip}(w_t^i(\theta^i), 1 - \epsilon, 1 + \epsilon) \hat{A}_t^i \right) \right],$$

$$\mathcal{L}_c^i = \mathbb{E}_t \left[\left(V^i(o_t^i; \phi^i) - \hat{R}_t^i \right)^2 \right],$$

where \hat{A}_t^i and \hat{R}_t^i are individual advantage and return for agent i at time step t , respectively. They are calculated locally as

$$\hat{A}_t^i = \sum_{t'=t}^{T-1} (\gamma\lambda)^{t'-t} \left(-V^i(o_{t'}^i; \phi^i) + r_{t'} + \gamma V^i(o_{t'+1}^i; \phi^i) \right),$$

$$\hat{R}_t^i = \hat{A}_t^i + V^i(o_t^i; \phi^i).$$

REFERENCES

- [1] Electric Power Annual 2019. [Online]. Available: <https://www.eia.gov/electricity/annual/>.
- [2] L. Yu, W. Xie, D. Xie, Y. Zou, D. Zhang, Z. Sun, L. Zhang, Y. Zhang, and T. Jiang, "Deep reinforcement learning for smart home energy management," *IEEE Internet of Things Journal*, vol. 7, no. 4, pp. 2751–2762, 2020.
- [3] L. Igualada, C. Corchero, M. Cruz-Zambrano, and F.-J. Heredia, "Optimal energy management for a residential microgrid including a vehicle-to-grid system," *IEEE Transactions on Smart Grid*, vol. 5, no. 4, pp. 2163–2172, 2014.
- [4] M. Ahmadi, J. M. Rosenberger, W.-J. Lee, and A. Kulvanitichaiyanunt, "Optimizing load control in a collaborative residential microgrid environment," *IEEE Transactions on Smart Grid*, vol. 6, no. 3, pp. 1196–1207, 2015.
- [5] H. Shuai and H. He, "Online scheduling of a residential microgrid via monte-carlo tree search and a learned model," *IEEE Transactions on Smart Grid*, vol. 12, no. 2, pp. 1073–1087, 2021.
- [6] O. Vinyals, I. Babuschkin, W. M. Czarnecki, M. Mathieu, A. Dudzik, J. Chung, D. H. Choi, R. Powell, T. Ewalds, P. Georgiev *et al.*, "Grandmaster level in starcraft ii using multi-agent reinforcement learning," *Nature*, vol. 575, no. 7782, pp. 350–354, 2019.
- [7] L. Yu, S. Qin, M. Zhang, C. Shen, T. Jiang, and X. Guan, "A review of deep reinforcement learning for smart building energy management," *IEEE Internet of Things Journal*, pp. 1–1, 2021.
- [8] C. Zhang, S. R. Kuppannagari, C. Xiong, R. Kannan, and V. K. Prasanna, "A cooperative multi-agent deep reinforcement learning framework for real-time residential load scheduling," in *Proceedings of the International Conference on Internet of Things Design and Implementation*, 2019, pp. 59–69.
- [9] J. Lee, W. Wang, and D. Niyato, "Demand-side scheduling based on multi-agent deep actor-critic learning for smart grids," in *2020 IEEE International Conference on Communications, Control, and Computing Technologies for Smart Grids (SmartGridComm)*, 2020, pp. 1–6.
- [10] L. Yu, Y. Sun, Z. Xu, C. Shen, D. Yue, T. Jiang, and X. Guan, "Multi-agent deep reinforcement learning for hvac control in commercial buildings," *IEEE Transactions on Smart Grid*, vol. 12, no. 1, pp. 407–419, 2021.
- [11] X. Xu, Y. Jia, Y. Xu, Z. Xu, S. Chai, and C. S. Lai, "A multi-agent reinforcement learning-based data-driven method for home energy management," *IEEE Transactions on Smart Grid*, vol. 11, no. 4, pp. 3201–3211, 2020.
- [12] H.-M. Chung, S. Maharjan, Y. Zhang, and F. Eliassen, "Distributed deep reinforcement learning for intelligent load scheduling in residential smart grids," *IEEE Transactions on Industrial Informatics*, vol. 17, no. 4, pp. 2752–2763, 2021.
- [13] A. Abdallah and X. S. Shen, "Lightweight authentication and privacy-preserving scheme for v2g connections," *IEEE Transactions on Vehicular Technology*, vol. 66, no. 3, pp. 2615–2629, 2017.
- [14] Z. Qin, D. Liu, H. Hua, and J. Cao, "Privacy preserving load control of residential microgrid via deep reinforcement learning," *IEEE Transactions on Smart Grid*, pp. 1–1, 2021.
- [15] A. Tampuu, T. Matiisen, D. Kodelja, I. Kuzovkin, K. Korjus, J. Aru, J. Aru, and R. Vicente, "Multiagent cooperation and competition with deep reinforcement learning," *PloS one*, vol. 12, no. 4, p. e0172395, 2017.
- [16] J. Foerster, G. Farquhar, T. Afouras, N. Nardelli, and S. Whiteson, "Counterfactual multi-agent policy gradients," in *Proceedings of the AAAI Conference on Artificial Intelligence*, vol. 32, no. 1, 2018.
- [17] Y. Du, H. Zandi, O. Kotevska, K. Kurte, J. Munk, K. Amasyali, E. Mckee, and F. Li, "Intelligent multi-zone residential hvac control strategy based on deep reinforcement learning," *Applied Energy*, vol. 281, p. 116117, 2021.
- [18] Y. Ye, D. Qiu, X. Wu, G. Strbac, and J. Ward, "Model-free real-time autonomous control for a residential multi-energy system using deep reinforcement learning," *IEEE Transactions on Smart Grid*, vol. 11, no. 4, pp. 3068–3082, 2020.
- [19] P. Sunehag, G. Lever, A. Gruslly, W. M. Czarnecki, V. Zambaldi, M. Jaderberg, M. Lanctot, N. Sonnerat, J. Z. Leibo, K. Tuyls *et al.*, "Value-decomposition networks for cooperative multi-agent learning based on team reward," in *Proceedings of the 17th International Conference on Autonomous Agents and MultiAgent Systems*, 2018, pp. 2085–2087.
- [20] T. Rashid, M. Samvelyan, C. Schroeder, G. Farquhar, J. Foerster, and S. Whiteson, "Qmix: Monotonic value function factorisation for deep multi-agent reinforcement learning," in *International Conference on Machine Learning*. PMLR, 2018, pp. 4295–4304.
- [21] M. Ahrarinnouri, M. Rastegar, and A. R. Seifi, "Multiagent reinforcement learning for energy management in residential buildings," *IEEE Transactions on Industrial Informatics*, vol. 17, no. 1, pp. 659–666, 2021.
- [22] R. Lowe, Y. WU, A. Tamar, J. Harb, O. Pieter Abbeel, and I. Mordatch, "Multi-agent actor-critic for mixed cooperative-competitive environments," *Advances in Neural Information Processing Systems*, vol. 30, pp. 6379–6390, 2017.
- [23] M. Zhou, Z. Liu, P. Sui, Y. Li, and Y. Y. Chung, "Learning implicit credit assignment for cooperative multi-agent reinforcement learning," *arXiv preprint arXiv:2007.02529*, 2020.
- [24] S. Iqbal and F. Sha, "Actor-attention-critic for multi-agent reinforcement learning," in *ICML*. PMLR, 2019, pp. 2961–2970.
- [25] Y. Wang, B. Han, T. Wang, H. Dong, and C. Zhang, "Dop: Off-policy multi-agent decomposed policy gradients," in *ICLR*, 2020.
- [26] A. K. Agogino and K. Tumer, "Unifying temporal and structural credit assignment problems," in *AAMAS*, vol. 4, 2004, pp. 980–987.
- [27] F. A. Oliehoek and C. Amato, *A concise introduction to decentralized POMDPs*. Springer, 2016.
- [28] K. Cho, B. van Merriënboer, Ç. Gülçehre, D. Bahdanau, F. Bougares, H. Schwenk, and Y. Bengio, "Learning phrase representations using rnn encoder-decoder for statistical machine translation," in *EMNLP*, 2014.
- [29] G. Panchal, A. Ganatra, Y. Kosta, and D. Panchal, "Behaviour analysis of multilayer perceptrons with multiple hidden neurons and hidden layers," *International Journal of Computer Theory and Engineering*, vol. 3, no. 2, pp. 332–337, 2011.
- [30] A. Sherstinsky, "Fundamentals of recurrent neural network (rnn) and long short-term memory (lstm) network," *Physica D: Nonlinear Phenomena*, vol. 404, p. 132306, 2020.

- [31] J. Schulman, F. Wolski, P. Dhariwal, A. Radford, and O. Klimov, "Proximal policy optimization algorithms," *arXiv preprint arXiv:1707.06347*, 2017.
- [32] V. Mnih, A. P. Badia, M. Mirza, A. Graves, T. Lillicrap, T. Harley, D. Silver, and K. Kavukcuoglu, "Asynchronous methods for deep reinforcement learning," in *International Conference on Machine Learning*. PMLR, 2016, pp. 1928–1937.
- [33] J. Schulman, P. Moritz, S. Levine, M. Jordan, and P. Abbeel, "High-dimensional continuous control using generalized advantage estimation," *arXiv preprint arXiv:1506.02438*, 2015.
- [34] T. P. Lillicrap, J. J. Hunt, A. Pritzel, N. Heess, T. Erez, Y. Tassa, D. Silver, and D. Wierstra, "Continuous control with deep reinforcement learning," *arXiv preprint arXiv:1509.02971*, 2015.
- [35] T. Haarnoja, A. Zhou, P. Abbeel, and S. Levine, "Soft actor-critic: Off-policy maximum entropy deep reinforcement learning with a stochastic actor," in *International Conference on Machine Learning*. PMLR, 2018, pp. 1861–1870.
- [36] G. Brockman, V. Cheung, L. Pettersson, J. Schneider, J. Schulman, J. Tang, and W. Zaremba, "Openai gym," 2016.
- [37] Pecan Street Database. [Online]. Available: <http://www.pecanstreet.org/>.
- [38] NOAA Data. [Online]. Available: <https://www.ncdc.noaa.gov/>.
- [39] D. P. Kingma and J. Ba, "Adam: A method for stochastic optimization," in *International Conference on Learning Representations*, 2015.



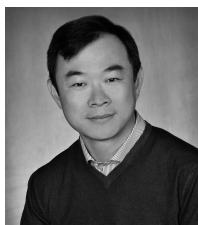
Junwei Cao is currently a Professor and the Vice Dean of the Research Institute of Information Technology, Tsinghua University, Beijing, China. He is also the Director of Open Platform and Technology Division, Tsinghua National Laboratory for Information Science and Technology. He received his PhD in Computer Science from the University of Warwick, Coventry, UK, in 2001. He received his bachelor and master degrees in Control Theories and Engineering in 1998 and 1996, respectively, both from Tsinghua University, Beijing, China. Prior to joining Tsinghua University in 2006, he was a Research Scientist at MIT LIGO Laboratory and NEC Laboratories Europe for about 5 years. He has published over 300 papers and cited by international scholars for over 66,000 times. He has authored or edited 8 books. His research focus on distributed computing technologies and energy/power applications. Prof. Cao is a Senior Member of the IEEE Computer Society and a Member of the ACM and CCF.



Zhaoming Qin is currently pursuing his master degree at the Department of Automation, Tsinghua University, Beijing, China. He received the B.Sc. in Automation from Beihang University, Beijing, China, in 2019. His current research focuses on reinforcement learning, specifically in the context of smart grids.



Nanqing Dong is currently a PhD student at the Department of Computer Science, University of Oxford, Oxford, UK. He received his master degree from the Department of Statistical Science, Cornell University, Ithaca, NY, USA, in 2017. Prior to Oxford, he worked at the Machine Learning Department, Carnegie Mellon University, Pittsburgh, PA, USA. His research interests include machine learning, computer vision, optimization, and quantum computing.



Eric P. Xing is a Professor at the Machine Learning Department, Carnegie Mellon University, Pittsburgh, PA, USA and the President of Mohamed bin Zayed University of Artificial Intelligence, Abu Dhabi, UAE. Prof. Xing received a PhD in Molecular Biology from Rutgers University, and another PhD in Computer Science from UC Berkeley. Prof. Xing is a recipient of the National Science Foundation (NSF) Career Award, the Alfred P. Sloan Research Fellowship in Computer Science, the United States Air Force Office of Scientific Research Young Investigator Award, the IBM Open Collaborative Research Faculty Award, as well as several best paper awards. Prof. Xing is a board member of the International Machine Learning Society. He is a Fellow of the Association of Advancement of Artificial Intelligence (AAAI), and an Institute of Electrical and Electronics Engineers (IEEE) Fellow. In the past, he served as the Program Chair (2014) and General Chair (2019) of the International Conference of Machine Learning (ICML). He is an associate editor of the *Annals of Applied Statistics* (AOAS), the *Journal of American Statistical Association* (JASA), the *IEEE Transaction of Pattern Analysis and Machine Intelligence* (PAMI), the *PLoS Journal of Computational Biology*, and an action editor of the *Machine Learning Journal* (MLJ), the *Journal of Machine Learning Research* (JMLR). He is a member of the DARPA Information Science and Technology (ISAT) Advisory Group.